

ASSESSING DIFFERENT SUPPORTS AND PROMOTERS FOR SULFUR RESILIENT METHANATION CATALYSTS AT LABORATORY SCALE

Manuel Bailera^{*1}, Carmen Bacariza², Paula Teixeira², Jorge Legaz³, Cristian Barón¹, Begoña Peña¹, Luis M. Romeo¹, Pilar Lisbona³

¹ Energy and CO₂ Group, Department of Mechanical Engineering, Aragon Institute of Engineering Research (I3A), University of Zaragoza, Zaragoza 50018, Spain

²Centro de Química Estrutural, Institute of Molecular Sciences, Departamento de Engenharia Química, Instituto Superior Técnico, Universidade de Lisboa, Portugal

³ Department of Mechanical Engineering, University of Zaragoza, Zaragoza 50018, Spain

*Corresponding Author: mbailera@unizar.es

ABSTRACT

Decarbonizing the industry is key to achieving goals against climate change. The use of synthetic fuels and their regeneration is promoted, utilizing the industry's own emissions. However, implementing processes like methanation for synthetic natural gas generation is a challenge in these industries due to the presence of impurities, especially problematic for catalysts, such as sulfur. The objective of this study is to compare different supports and promoters for a nickel-based methanation catalyst at various levels of sulfur poisoning (0 - 1 wt%). Additionally, a sulfur-dependent kinetic model was developed for the best Ni/Support catalyst. Based on the results obtained, alumina emerged as the optimal catalyst support, showcasing superior catalytic performance compared to other tested materials across all examined reaction temperatures. Additionally, calcium (1 wt.%) was identified as the most effective promoter, demonstrating the highest performance not only in unpoisoned catalysts but also when comparing samples with 1 wt.% of sulfur.

1 INTRODUCTION

The Sabatier reaction, also known as CO₂ methanation, is a promising method for converting industrial flue gases containing carbon dioxide into synthetic natural gas. Although there have been numerous research studies reporting highly active, selective, and stable catalysts towards the Sabatier reaction, mostly containing Ni or Ru as active metals and metal oxides, carbons, zeolites, metal-organic frameworks, or hydrotalcites as support (Ashok *et al.*, 2020; Bacariza *et al.*, 2020; Lv *et al.*, 2020; Lee *et al.*, 2021), few publications have analyzed the effects of adding typical flue gases' minor compounds, such as sulfur, to the feed (Yuan *et al.*, 2015; Alarcon *et al.*, 2019; Guilera *et al.*, 2019; Wolf, Schüler and Hinrichsen, 2019; Méndez-Mateos *et al.*, 2020; Wolf *et al.*, 2020; Dou *et al.*, 2021; Cimino, Cepollaro and Lisi, 2022).

Ni-based catalysts are the most commonly used catalysts for industrial scale methanation. However, due to the presence of sulphur in industrial flue gas (like in ironmaking, **Table 1**), nickel is easily poisoned due to the formation of NiS compounds that deactivate Ni⁰ active centers. Surface sulphide species formation reduces the number of available active sites for H₂ dissociation and CO₂ activation, leading to a poisoning effect rather than a kinetic or mechanistic one. Additionally, sulfur promotes the formation of carbon deposits and the sintering of metal particles.

To reduce the negative impact of sulfur poisoning on Ni catalysts' performance towards CO₂ methanation, previous studies have reported incorporating noble and transition metals, rare-earth metal oxides, or alkali/alkali-earth metal oxides in their formulation. Recently, modified catalysts that include rare earth promoters such as cerium or alkaline species have been shown to prevent S-poisoning. (Yuan

et al., 2015; Alarcon *et al.*, 2019; Guilera *et al.*, 2019; Wolf, Schüler and Hinrichsen, 2019; Méndez-Mateos *et al.*, 2020; Wolf *et al.*, 2020; Dou *et al.*, 2021; Cimino, Cepollaro and Lisi, 2022).

Table 1. Sulfur compounds in blast furnace gas before and after treatment.

Compound	Untreated gas (mg/Nm ³)	Treated gas (mg/Nm ³)
COS	80 – 300	0.8 – 3
H ₂ S	5 – 70	0 – 37
SO ₂	0.2 – 12	0 – 1.2

In this article, a study is presented to select the best support and promoter for the methanation of CO₂, including situations of sulfur poisoning. Additionally, kinetic equations for Ni/Al₂O₃ have been developed for the first time, which are dependent on the amount of sulfur adsorbed on the catalyst. The kinetics are valid for poisonings ranging from 0 to 1 wt.% of sulfur.

2 METHODS

2.1 Catalyst preparation

A total of 9 different catalyst were prepared (**Table 2**): 4 of them to assess the effect of the support (Commercial HUSY zeolite, Al₂O₃, CeO₂ and La₂O₃), and 5 to assess the effect of promoters (Ru, Fe, Co, Mo or Ca). Despite Alumina is already a well-known support for catalyst, a comparison with other supports is made in order to check if any of them provide better activity against sulfur poisoning. The catalysts were synthesized by incipient wetness impregnation using nitrate precursor salts followed by calcination under air flow (60 ml/min/g; heating rate of 2 °C/min) at 200 °C (1 h) and 500 °C (6 h). The Ni content was 13 wt% in all of them, and the promoters content was set at 1 wt%.

To study the sulfur effect on the catalysts, all catalysts were ex-situ poisoned with 1 wt.% S. For this purpose, calcined catalysts were impregnated with an aqueous solution of diluted ammonium sulphide followed by drying at 80 °C for 18 h in an oven. Afterwards, a thermal treatment was performed at 470 °C (3 °C/min) under H₂/N₂ flow (80/20; 60 ml/min/g) for 1 h. This strategy for evaluating S effect on catalysts performance, reported by Wolf *et al.* (Wolf, Schüler and Hinrichsen, 2019), intended to simulate the state of the materials after being submitted to a S-containing stream for a certain period of time, thus acting as a forced aging. The loading of 1 wt.% S was initially chosen based on the analysis of literature for spent catalysts tested using H₂S or SO₂-containing feeds (Yuan *et al.*, 2015; Cimino, Cepollaro and Lisi, 2022) as well as on the loadings used by Wolf *et al.* (Wolf, Schüler and Hinrichsen, 2019). Additionally, the Ni/Al₂O₃ catalyst was selected to be tested using additional sulphur loadings, covering: 0.0 - 1.0 wt.%.

Table 2. Catalyst synthesized

Study	Catalyst	Ni (wt%)	Promoter (wt%)	S (wt%)
Support	Ni/HY	13	-	0.0 and 1.0
	Ni/Al ₂ O ₃			
	Ni/CeO ₂			
	Ni/La ₂ O ₃			
Promoter	NiRu/Al ₂ O ₃	13	1	0.0 and 1.0
	NiFe/Al ₂ O ₃			
	NiCo/Al ₂ O ₃			
	NiMo/Al ₂ O ₃			
Kinetics	NiCa/Al ₂ O ₃	13	-	0.0, 0.2, 0.5, 0.7 and 1.0
	Ni/Al ₂ O ₃			

2.2 Catalyst characterization

Catalysts were characterized by powder XRD, H₂-TPR, N₂ sorption and elemental analysis. Powder XRD patterns were collected using a Bruker AXS Advance D8 diffractometer equipped with a 1D detector (SSD 160) and using a Ni filter. Each sample was scanned within the 2 θ range of 5–80 °, with a step size of 0.03 ° and a step time of 0.5 s. The H₂-TPR profiles were obtained in an AutoChem II equipment from Micromeritics from room temperature to 900 °C under a 5 % H₂/Ar flow and a mass of catalyst of ~0.150 g. The N₂ sorption was carried out on an Autosorb iQ equipment (Quantachrome) at -196 °C. The catalysts were degassed under vacuum prior to the experiments at 90 °C (1 h) and 350 °C (4 h). Micropores volumes and external surface areas were obtained from t-plot method. Total pore volumes were measured at a relative pressure of 0.95. Mesopores volumes were determined as the difference between the total pore volumes and the micropores volume. Elemental analysis for Ni, Fe, Co, Mo and Ca contents was performed at Laboratório Central de Análises (Universidade de Aveiro, Portugal), while S loading was determined at Centro de Investigação CERES (Universidade de Coimbra, Portugal). Additional SEM-EDS analyses were performed at MicroLab (Instituto Superior Técnico, Portugal) to confirm the presence of S in the poisoned samples.

2.3 Experimental setup

The catalytic tests were performed at 1 bar from 200 to 450 °C, increasing the temperature by steps of 25 °C, using a homemade unit (Figure 1). A fixed-bed reactor presenting a porous glass filter where 0.200 g of catalyst in powder form were loaded was used. Unpoisoned catalysts were in-situ pre-reduced at 470 °C before reaction (2.5 °C/min, molar ratio of H₂:N₂ = 4:1, total flow of 250 mL min⁻¹). Catalysts containing sulphur were ex-situ pre-reduced to avoid any sulphur contamination in the catalytic setup. For the reaction, a mixture of H₂, CO₂ and N₂ (inert) was used (molar ratio of H₂:CO₂:N₂ = 36:9:10, total flow of 287 mL min⁻¹). The reactor effluent was analysed using Guardian® NG infrared detectors (Edinburgh Sensors) for CO₂, CH₄ and CO, and outlet flows were measured for each temperature after reaching steady state. The corresponding CO₂, CH₄ and CO molar flows were determined, being CO₂ conversions, CH₄ selectivity and CH₄ yields calculated for each temperature. The selection of the pressure (1 bar) is based on the limitations of a second experimental setup of larger scale (1 kW), with which we intend to compare results in a later study.

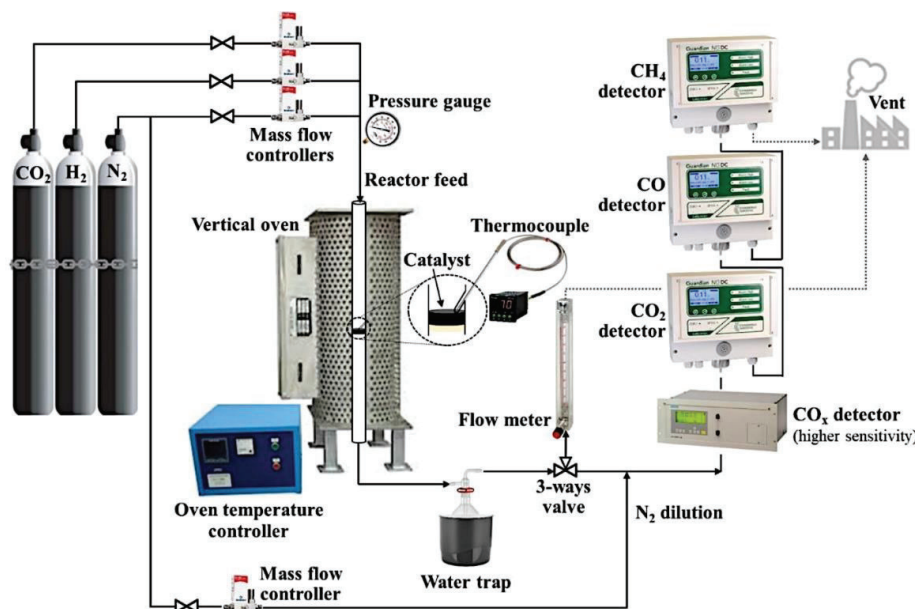


Figure 1. Scheme of the installation used for catalytic testing.

2.4 Kinetic model adjustment

A kinetic model was elaborated for the Ni/Al₂O₃ catalyst, aiming to cover all the experimental results of the different sulfur loadings (from 0.0 to 1.0 wt% S). The model was based in the kinetics proposed by Xu and Froment (Eq.(1) and (2)) for the reactions in Eq.(3) and (4) (Xu and Froment, 1989).

$$r_1 = \frac{\frac{k_1}{p_{H_2}} \left(p_{CO} p_{H_2O} - \frac{p_{CO_2} p_{H_2}}{K_{eq1}} \right)}{\left(1 + K_{CO} p_{CO} + K_{H_2} p_{H_2} + K_{CH_4} p_{CH_4} + \frac{K_{H_2O} p_{H_2O}}{p_{H_2}} \right)^2} \quad (1)$$

$$r_2 = \frac{\frac{k_2}{p_{H_2}^{2.5}} \left(p_{CH_4} p_{H_2O} - \frac{p_{CO} p_{H_2}^3}{K_{eq2}} \right)}{\left(1 + K_{CO} p_{CO} + K_{H_2} p_{H_2} + K_{CH_4} p_{CH_4} + \frac{K_{H_2O} p_{H_2O}}{p_{H_2}} \right)^2} \quad (2)$$



The terms p_i are the partial pressures of the components, k_i is the rate coefficient (Eq.(5), Arrhenius equation), K_{eq} is the equilibrium constant (Eq.(6) and (7)), and K_i are the adsorption constants of each component (Eq.(8)).

$$k_i = k_{i,0} \cdot \exp\left(-\frac{E_{A,i}}{R \cdot T}\right) \quad (5)$$

$$K_{eq1} = \exp\left(\frac{4400}{T} - 4.063\right) \quad (6)$$

$$K_{eq2} = 1.026676 \times 10^{10} \exp\left(\frac{-26830}{T} + 30.11\right) \quad (7)$$

$$K_i = K_{i,0} \cdot \exp\left(-\frac{\Delta H_i^0}{R \cdot T}\right) \quad (8)$$

The parameters $k_{i,0}$ (pre-exponential factor), $E_{A,i}$ (activation energy), $K_{i,0}$ (adsorption constants, and ΔH_i^0 (enthalpies of adsorption) were obtained by minimizing the arithmetic mean (Eq.(9)) of the mean squared error (MSE) for the CO₂ conversion (Eq.(10)) and for the CH₄ selectivity (Eq.(11)), over a number of tests N . The CO₂ conversion and the CH₄ selectivity are defined according to Eq.(12) and (13), where $\dot{n}_{i,0}$ is the mole flow of component i at the inlet, and \dot{n}_i at the outlet.

$$M_{MSE} = \frac{MSE_x + MSE_s}{2} \quad (9)$$

$$MSE_x = \sqrt{\frac{\sum_j^N (x_{CO_2,j}^{model} - x_{CO_2,j}^{test})^2}{N}} \quad (10)$$

$$MSE_s = \sqrt{\frac{\sum_j^N (s_{CH_4,j}^{model} - s_{CH_4,j}^{test})^2}{N}} \quad (11)$$

$$x_{CO_2} = \frac{\dot{n}_{CO_2,0} - \dot{n}_{CO_2}}{\dot{n}_{CO_2,0}} 100 \quad (12)$$

$$s_{\text{CH}_4} = \frac{\dot{n}_{\text{CH}_4}}{\dot{n}_{\text{CH}_4} + \dot{n}_{\text{CO}}} 100 \quad (13)$$

The M_{MSE} was minimized by using the Powell Method (Vassiliadis and Conejeros, 2008). First, the data of each sulfur poisoning was adjusted separately (0.0, 0.2, 0.5, 0.7 and 1.0 wt.% S), therefore obtaining five different models. Then, the parameters $k_{i,0}$, $E_{A,i}$ and ΔH_i^0 of each model were fitted to S-dependent functions by the least squares method. Lastly, as final iteration, the M_{MSE} was minimized again via the Powell Method by letting free the parameters of the S-dependent functions. Half of the experimental data was used for adjusting the kinetic model, and the other half was used for validating the model.

3 RESULTS AND DISCUSSION

3.1 Support nature effect

Ni/Support catalysts, both unpoisoned and poisoned, were tested for CO₂ methanation under previously described conditions. **Figure 2** presents the CO₂ conversions and CH₄ selectivity for Ni/Support samples. The performance of unpoisoned catalysts followed the order: Ni/Al₂O₃ >> Ni/HY > Ni/CeO₂ ≈ Ni/La₂O₃. The better performance of Ni/Al₂O₃ is justified by the smaller Ni⁰ crystallite sizes (observed by XRD), the higher CO₂ adsorption capacity (Quindimil *et al.*, 2021), the stronger metal-support interactions (observed by H₂-TPR) and the higher textural properties (observed by N₂ sorption). In the case of Ni/CeO₂, the poorer activity may be caused by the largest Ni⁰ particles and the weaker metal-support interactions found. However, to gain a better understanding of the catalysts' activity, it is necessary to explore other properties such as hydrophobicity. This is expected to be higher in the case of Ni/HY, which may explain its intermediate performance.

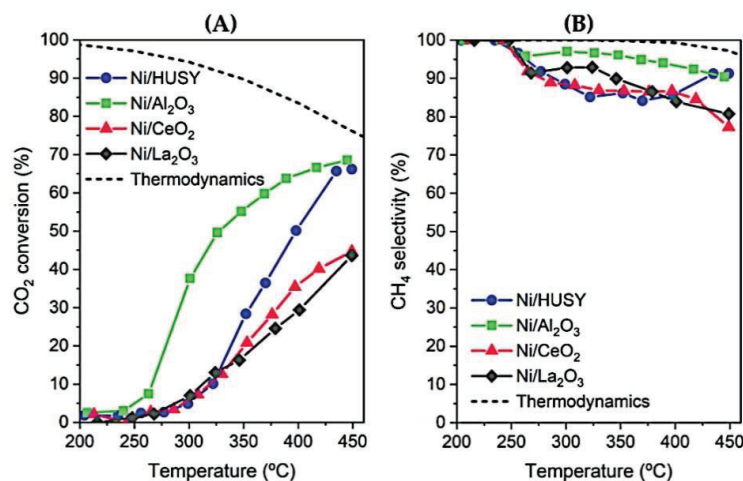


Figure 2. Catalytic performances obtained for Ni/HY, Ni/Al₂O₃, Ni/CeO₂ and Ni/La₂O₃ catalysts after reduction at 470 °C: (A) CO₂ conversion; (B) CH₄ selectivity. Operating conditions: 1 bar, 86 100 mL h⁻¹ gcat⁻¹ and CO₂:H₂:N₂ = 9:36:10.

Figure 3 presents the catalytic performances of poisoned catalysts (Ni/Support_1S). It is observed that all catalysts exhibited poor performance in the studied temperature range, with CO₂ conversion below 20% (**Figure 3 A**) and CH₄ selectivity considerably lower than those from unpoisoned samples (**Figure 3 B**). **Figure 4** analyses the effect of S addition on CO₂ conversions at 350 °C. The performance of all catalysts decreased drastically in the presence of 1 wt.% S, with Ni/CeO₂, HY, Al₂O₃, and La₂O₃ experiencing reductions of 96%, 91%, 90%, and 67%, respectively. Overall, the highest CO₂ conversion values were achieved with Ni/Al₂O₃ and Ni/La₂O₃. Due to the lower cost and higher availability of Al₂O₃, this support was selected to perform the promoter effect study.

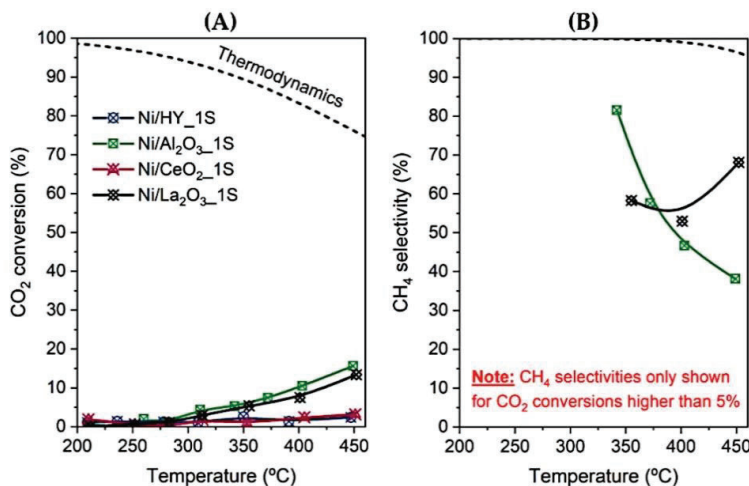


Figure 3. Catalytic performances obtained for Ni/HY_1S, Ni/Al₂O₃_1S, Ni/CeO₂_1S and Ni/La₂O₃_1S catalysts after reduction at 470 °C: (A) CO₂ conversion; (B) CH₄ selectivity. Operating conditions: 1 bar, 86 100 mL h⁻¹ gcat⁻¹ and CO₂:H₂:N₂ = 9:36:10.

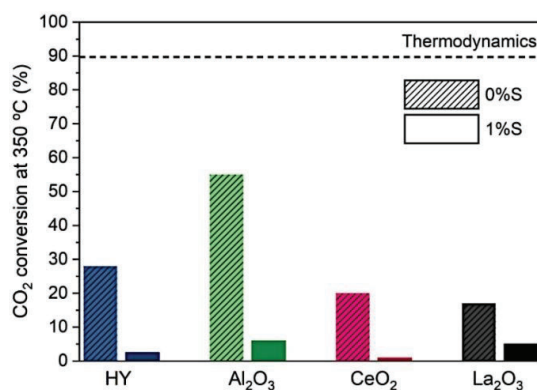


Figure 4. CO₂ conversion at 400 °C of unpoisoned and poisoned (1 wt.% S) Ni/HY, Ni/Al₂O₃, Ni/CeO₂ and Ni/La₂O₃ catalysts.

3.2 Promoter nature effect

Figure 5 shows the CO₂ conversion and CH₄ selectivity of unpoisoned NiP/Al₂O₃ catalysts. The results follow the trend NiCa/Al₂O₃ > NiCo/Al₂O₃ > NiRu/Al₂O₃ > NiFe/Al₂O₃ > Ni/Al₂O₃ > NiMo/Al₂O₃. Co and Ca significantly enhanced CO₂ conversion. The CO₂ conversion increased from 55% without a promoter to 73% and 72% with Co and Ca, respectively, while maintaining CH₄ yields around 70% at 350 °C. The positive effect of Ca could arise from an improved Ni reducibility, basicity, and nickel particle dispersion (Bacariza *et al.*, 2021; Sabokmalek *et al.*, 2023). The good performance of Co and Ru may come from the ability to dissociate H₂ molecules (and CO₂ molecules in the case of Ru), contributing to this step of the reaction mechanism (Quindimil *et al.*, 2021). In the case of Fe, the formation of NiFe alloys was reported to improve nickel metallic dispersion and lead to synergistic effects (Tsiotsias *et al.*, 2020). Finally, some studies reported that Mo is favourable for Ni catalysts towards CO₂ methanation (Aksoylu, Mısırlı and Önsan, 1998), but it does not seem to have a positive impact on the catalyst properties in this study.

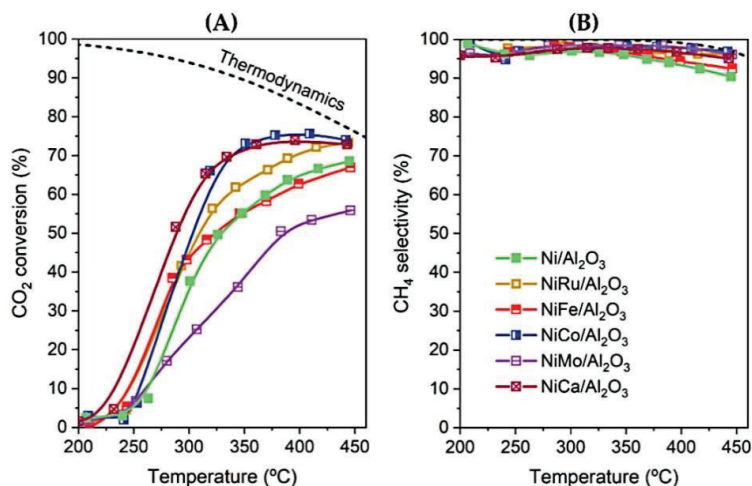


Figure 5. Catalytic performances for NiP/Al₂O₃ after reduction at 470 °C: (A) CO₂ conversion; (B) CH₄ selectivity. Operating conditions: 1 bar, 86100 mL h⁻¹ gcat⁻¹ and CO₂:H₂:N₂ = 9:36:10.

Regarding the effect of 1 wt.% sulfur incorporation (**Figure 6**), the results show that, similar to Ni/Support catalysts, this compound causes a significant decrease in catalytic performance within the studied temperature range.

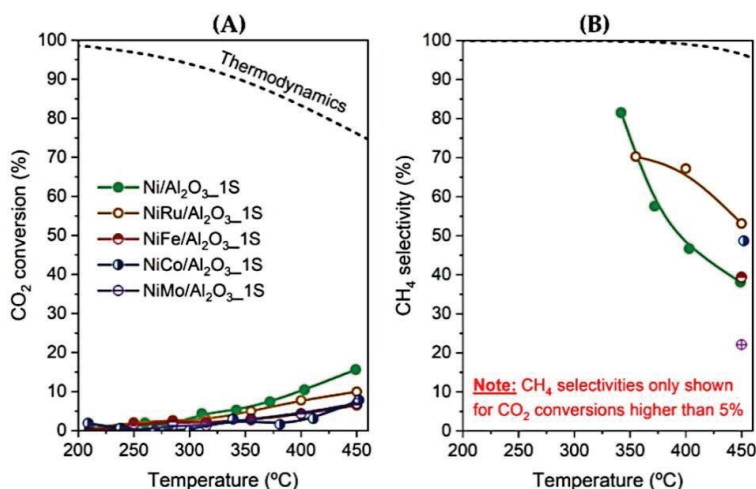


Figure 6. Catalytic performances obtained for for NiP/Al₂O₃_1S catalysts after reduction at 470 °C: (A) CO₂ conversion; (B) CH₄ selectivity. Operating conditions: 1 bar, 86 100 mL h⁻¹ gcat⁻¹ and CO₂:H₂:N₂ = 9:36:10.

Figure 7 presents the CO₂ conversion for unpoisoned and poisoned promoted catalysts at 350°C. Despite the promoters' advantages under conventional conditions, the catalysts' deactivation was remarkably accentuated in the presence of 1% sulphur. Among the 5 studied promoters, Ru and Ca showed a higher deactivation resistance to sulphur. Given the lower price and availability of Ca, this is recommended as the best potential candidate for further investigation.

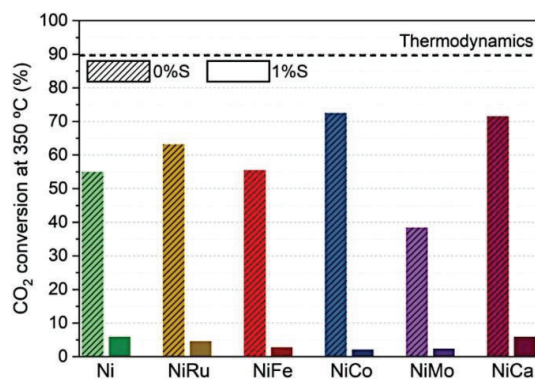


Figure 7. CO₂ conversion at 350 °C of unpoisoned and poisoned (1% of sulphur) Ni/Al₂O₃; NiRu/Al₂O₃; NiFe/Al₂O₃; NiCo/Al₂O₃; NiMo/Al₂O₃ and NiCa/Al₂O₃ catalysts.

3.3 Sulfur loading effect

Figure 8 presents the CO₂ conversion and CH₄ selectivity for Ni/Al₂O₃ catalyst after incorporating different S loadings. The results show how the catalyst experienced deactivation as S loadings increased. Even with the lowest tested content (0.2 wt.% S), CO₂ conversion decreased significantly (from 55% to 31%, at 350 °C). Nevertheless, this was not accompanied by a significant reduction in selectivity towards methane (decreased from 96% to 93%). This suggests that the effect of S poisoning on catalysts' active sites is limited. Further increases in sulphur incorporation, simulating longer exposure of the catalyst to a sulphur-containing stream, significantly affected both CO₂ conversion and CH₄ selectivity. This indicates that the functionalities of the catalyst were significantly compromised beyond 0.5 wt.% S.

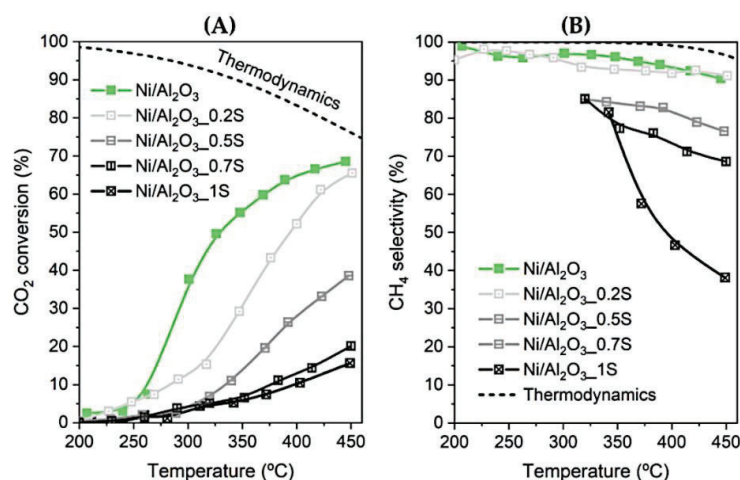


Figure 8. Catalytic performances obtained for the Ni/Al₂O₃ catalyst unpoisoned and poisoned with 0.2, 0.5, 0.7 and 1 wt.% of sulphur, after reduction at 470 °C: (A) CO₂ conversion; (B) CH₄ selectivity.

Operating conditions: 1 bar, 86 100 mL h⁻¹ gcat⁻¹ and CO₂:H₂:N₂ = 9:36:10.

3.4 Sulfur-dependent kinetics

Table 3 shows the parameters for the fitted kinetic equations, including their dependence on the percentage of sulfur in the catalyst. This model is the first in the literature that is valid for a poisoning process. The model is valid under the following operating conditions: 0.0 – 1.0 wt.% S poisoning, 1 bar, 200 – 450 °C, and 86 100 mL h⁻¹ gcat⁻¹.

Table 3. Parameters of the sulfur-dependent kinetics for the CO₂ methanation via Ni/Al₂O₃ catalyst (S is the weight percentage of sulfur in the catalyst (%)). Valid for: 0.0 – 1.0 wt.% S poisoning, 1 bar, 200 – 450 °C, and 86 100 mL h⁻¹ gcat⁻¹.

Parameter	Units
$k_{1,0} = \left(0.00072 + \exp\left(\frac{-S}{0.0379407}\right)\right)S + (1 - S) \exp(6.02342 - 10.06121 S - 33.42 S^2)$	mol/(g _{cat} S Pa)
$k_{2,0} = 6.673 \times (1 - 0.009588 \times S) \times 10^{12}$	mol Pa ^{0.5} /(g _{cat} S)
$E_{A,1} = 78758 + 135817 S + 1204210 S^2 + 1949110 S^3 - 909443 S^4$	J/mol
$E_{A,2} = 205843 + 18747 S$	J/mol
$K_{CO,0} = 6.4 \times 10^{-16}$	1/Pa
$K_{H_2,0} = 1.2 \times 10^{-17}$	1/Pa
$K_{CH_4,0} = 1.05048 \times 10^{-5}$	1/Pa
$K_{H_2O,0} = 245939$	-
$\Delta H_{CO}^0 = 0$	J/mol
$\Delta H_{H_2}^0 = -115408 + 88885 S + 113593 S^2$	J/mol
$\Delta H_{CH_4}^0 = -27133 - 11452 S - 23471 S^2 + 33795 S^3$	J/mol
$\Delta H_{H_2O}^0 = 501969 + 350967 S - 1060270 S^2 + 992534 S^3 - 286057 S^4$	J/mol

To fit the model, 24 out of the 47 experimental data points were used (see **Figure 9**, A1 and A2). The remaining 23 tests were used to verify the validity of the fitted model (see **Figure 9**, V1 and V2). Figure 9 shows a comparison between the theoretical results of the fitted model and the experimental results, with the discrepancy remaining within the range ±10%.

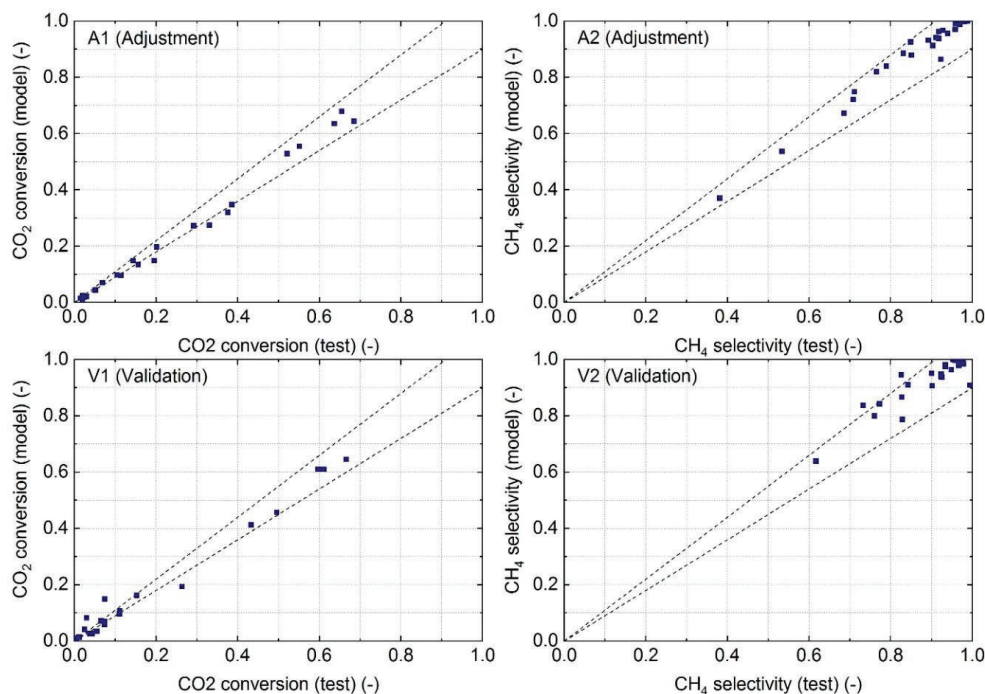


Figure 9. Comparison on CO₂ conversion and CH₄ selectivity between model and tests for Ni/Al₂O₃ in the range of S poisoning 0.0 – 1.0 wt.% S: (A1) and (A2) data used to adjust the kinetics, (V1) and (V2) data not involved in the kinetics adjustment, thus validating the model.

Figure 10 shows a comparison of conversion versus temperature for different levels of poisoning, both theoretically and experimentally. The model and tests demonstrate a good fit, with the catalyst progressively deactivating at higher levels of poisoning. If the poisoning were characterized as a function of time, it could be substituted into the parameters dependent on S, creating a model that predicts real-time conversion.

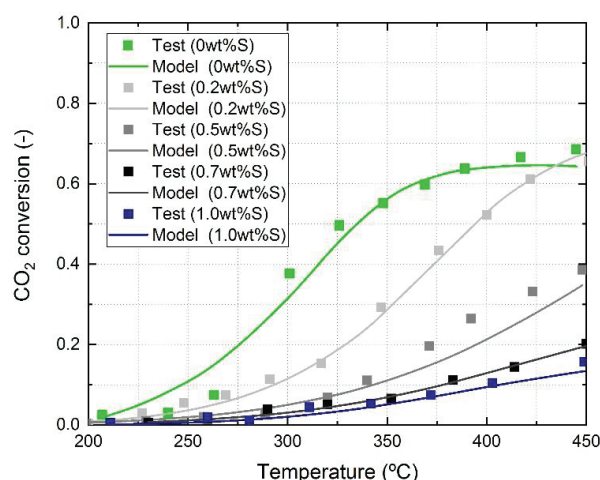


Figure 10. Comparison on CO₂ conversion between model and test results for Ni/Al₂O₃ (0.0 – 1.0 wt.% S). Operating conditions: 1 bar, 86 100 mL h⁻¹ gcat⁻¹ and CO₂:H₂:N₂ = 9:36:10

4 CONCLUSIONS

This paper presents three studies aimed at obtaining active and selective catalysts for CO₂ methanation in S-containing streams. The first study identifies a promising and available catalyst support, while the second identifies a well-performing and cost-efficient promoter. The third study tests the effect of variable S loadings on the performance of the best Ni/Support catalysts. Finally, the results are adjusted to a S-dependent kinetic model.

Alumina was identified as the best catalyst support based on the obtained results, displaying higher catalytic performance than the other tested materials at all reaction temperatures. Furthermore, the study found that the addition of 1 wt.% calcium was the most effective promoter, resulting in superior performance in both unpoisoned and 1 wt.% S-containing catalysts. The study highlighted the advantageous metal-support interactions, the CO₂ adsorption capability of alumina, and the notably improved Ni⁰ crystallite size as the key factors responsible for the superior performance of Ni/Al₂O₃. Furthermore, according to literature, the inclusion of calcium can enhance the CO₂ adsorption capacity and improve the dispersion of metals in the catalysts, which may account for its positive impact on the outcomes.

Finally, the catalyst Ni/Al₂O₃ was tested with variable S loadings (0.2, 0.5, 0.7 and 1 wt.%). It was observed that the catalyst showed better tolerance towards sulphur deposition at lower S amounts (0.2 wt.%), with activities decreasing drastically for increasing contents. The kinetic model developed provides a good agreement with experimental test, valid for 0.0 – 1.0 wt.% S poisoning, 1 bar, 200 – 450 °C, and 86 100 mL h⁻¹ gcat⁻¹. This is the first CO₂ methanation kinetic model that includes the dependency with the sulfur poisoning.

NOMENCLATURE

ΔH_i^0	J/mol	Enthalpy of adsorption
$E_{A,i}$	J/mol	Activation energy of reaction
k_1	mol/(g _{cat} s Pa)	Rate coefficient of reaction
$k_{1,0}$	mol/(g _{cat} s Pa)	Preexponential factor of rate coefficient
k_2	mol Pa ^{0.5} /(g _{cat} s)	Rate coefficient of reaction
$k_{2,0}$	mol Pa ^{0.5} /(g _{cat} s)	Preexponential factor of rate coefficient
$K_{eq,1}$	-	Equilibrium constant
$K_{eq,2}$	Pa ²	Equilibrium constant
K_i	1/Pa or -	Adsorption constant
$K_{i,0}$	1/Pa or -	Preexponential factor of adsorption constant
M_{MSE}	pp	Mean value of Mean squared errors
MSE_x	pp	Mean squared error
\dot{n}_i	mol/s	Mole flow at the outlet of the reactor
$\dot{n}_{i,0}$	mol/s	Mole flow at the inlet of the reactor
N	-	Number of tests
p_i	Pa	Pressure
r_i	mol/(g _{cat} s)	Rate of reaction
R	J/(mol K)	Gas constant
S_{CH4}	%	Selectivity towards methane
S	%	Sulfur weight content in catalyst
T	K	Temperature
x_{CO2}	%	CO ₂ conversion

REFERENCES

- Aksoylu, A. E., Mısırlı, Z. and Önsan, Z. İ. (1998) 'Interaction between nickel and molybdenum in Ni-Mo/Al₂O₃ catalysts: I', *Applied Catalysis A: General*, 168(2), pp. 385–397. doi: 10.1016/S0926-860X(97)00369-4.
- Alarcon, A. *et al.* (2019) 'Higher tolerance to sulfur poisoning in CO₂ methanation by the presence of CeO₂'. doi: 10.1016/j.apcatb.2019.118346.
- Ashok, J. *et al.* (2020) 'A review of recent catalyst advances in CO₂ methanation processes', *Catalysis Today*. Elsevier B.V., 356, pp. 471–489. doi: 10.1016/j.cattod.2020.07.023.
- Bacariza, M. C. *et al.* (2020) 'Promising Catalytic Systems for CO₂ Hydrogenation into CH₄: A Review of Recent Studies', *Processes*, 8(12), p. 1646. doi: 10.3390/pr8121646.
- Bacariza, M. C. *et al.* (2021) 'Alkali and Alkali-Earth Metals Incorporation to Ni/USY Catalysts for CO₂ Methanation: The Effect of the Metal Nature', *Processes*, 9(10), p. 1846. doi: 10.3390/pr9101846.
- Cimino, S., Cepollaro, E. M. and Lisi, L. (2022) 'Sulfur tolerance and self-regeneration mechanism of Na-Ru/Al₂O₃ dual function material during the cyclic CO₂ capture and catalytic methanation', *Applied Catalysis B: Environmental*, 317, p. 121705. doi: 10.1016/j.apcatb.2022.121705.
- Dou, L. *et al.* (2021) 'Efficient sulfur resistance of Fe, La and Ce doped hierarchically structured catalysts for low-temperature methanation integrated with electric internal heating', *Fuel*, 283, p. 118984. doi: 10.1016/j.fuel.2020.118984.
- Guilera, J. *et al.* (2019) 'Metal-oxide promoted Ni/Al₂O₃ as CO₂ methanation micro-size catalysts', *Journal of CO₂ Utilization*, 30, pp. 11–17. doi: https://doi.org/10.1016/j.jcou.2019.01.003.
- Lee, W. J. *et al.* (2021) 'Recent trend in thermal catalytic low temperature CO₂ methanation: A critical review', *Catalysis Today*. Elsevier B.V., 368(November 2019), pp. 2–19. doi: 10.1016/j.cattod.2020.02.017.
- Lv, C. *et al.* (2020) 'Recent Progresses in Constructing the Highly Efficient Ni Based Catalysts With Advanced Low-Temperature Activity Toward CO₂ Methanation', *Frontiers in Chemistry*, 8. doi:

- 10.3389/fchem.2020.00269.
- Méndez-Mateos, D. *et al.* (2020) ‘A study of deactivation by H₂S and regeneration of a Ni catalyst supported on Al₂O₃, during methanation of CO₂. Effect of the promoters Co, Cr, Fe and Mo’, *RSC Advances*, 10(28), pp. 16551–16564. doi: 10.1039/d0ra00882f.
- Quindimil, A. *et al.* (2021) ‘Enhancing the CO₂ methanation activity of γ -Al₂O₃ supported mono- and bi-metallic catalysts prepared by glycerol assisted impregnation’, *Applied Catalysis B: Environmental*, 296, p. 120322. doi: 10.1016/j.apcatb.2021.120322.
- Sabokmalek, S. *et al.* (2023) ‘Hydrogen Production by Glycerol Steam Reforming on the Ni/CaO-Al₂O₃ Catalysts: The Study of Synergistic Effect Between CaO and Al₂O₃’, *Catalysis Letters*, 153(12), pp. 3698–3711. doi: 10.1007/s10562-022-04247-1.
- Tsiotsias, A. I. *et al.* (2020) ‘Bimetallic Ni-Based Catalysts for CO₂ Methanation: A Review’, *Nanomaterials*, 11(1), p. 28. doi: 10.3390/nano11010028.
- Vassiliadis, V. S. and Conejeros, R. (2008) ‘Powell Method’, in *Encyclopedia of Optimization*. Boston, MA: Springer US, pp. 3012–3013. doi: 10.1007/978-0-387-74759-0_516.
- Wolf, M. *et al.* (2020) ‘CO₂ methanation on transition-metal-promoted Ni-Al catalysts: Sulfur poisoning and the role of CO₂ adsorption capacity for catalyst activity’, *Journal of CO₂ Utilization*, 36(October 2019), pp. 276–287. doi: 10.1016/j.jcou.2019.10.014.
- Wolf, M., Schüller, C. and Hinrichsen, O. (2019) ‘Sulfur poisoning of co-precipitated Ni–Al catalysts for the methanation of CO₂’, *Journal of CO₂ Utilization*, 32, pp. 80–91. doi: 10.1016/j.jcou.2019.03.003.
- Xu, J. and Froment, G. F. (1989) ‘Methane steam reforming, methanation and water-gas shift: I. Intrinsic kinetics’, *AIChE Journal*, 35(1), pp. 88–96. doi: 10.1002/aic.690350109.
- Yuan, C. *et al.* (2015) ‘The SiO₂ supported bimetallic Ni–Ru particles: A good sulfur-tolerant catalyst for methanation reaction’, *Chemical Engineering Journal*, 260, pp. 1–10. doi: 10.1016/j.cej.2014.08.079.

ACKNOWLEDGEMENT

This publication is supported by RYC2022-038283-I, funded by MCIN/ AEI/ 10.13039/ 501100011033 and the European Social Fund Plus (FSE+). This work is also part of the R&D project TED2021-130000B-I00, funded by MCIN/ AEI/ 10.13039/ 501100011033/ and by the “European Union NextGenerationEU/PRTR”. The publication was also supported by Centro de Química Estructural (UIDB/00100/2020, UIDP/00100/2020), and the Institute of Molecular Sciences (LA/P/0056/2020), both funded by FCT.